# Pain Expectations: the neural representations of predicted pain in self and others

L. Loued-Khenissi[1,2], G. A. Bergmann[3,2], C. Corradi-Dell'Acqua[4,2]

1.Department of Clinical Neurosciences, Lausanne University Hospital, Lausanne University

2. Theory of Pain Laboratory, Department of Psychology, Faculty of Psychology and Educational Sciences (FPSE), University of Geneva, Geneva 1202, Switzerland

3. Department of Economics, University of Zurich

4. Center for Mind/Brain Sciences (CIMeC), University of Trento, 38068 Rovereto, Italy.

**Abstract**

Predicting another's pain is a challenging decision. Predictive coding explains individual pain via top-down modulation, but its extension to vicarious pain is unknown. We tested neural representations of expected pain, uncertainty (risk), and their related errors for self versus other to assess predictive coding's explanatory power in decisions on another's pain. We hypothesized that the brain encodes expected pain, risk, and prediction errors for others, mirroring self-pain mechanisms within a predictive coding framework. Using model-based fMRI (n=33), individuals in dyads gambled on risky or certain pain relief; priced their choices; experienced or witnessed corollary pain, and rated the latter's intensity, alternating between deciding for themselves or another. Behaviorally, prosocial biases emerged in the form of greater risk aversion, higher pain relief valuation, and inflated ratings for others. Neurally, expected other-pain showed a graded representation (absent for self). Pain risk activated the dorsal striatum for both self and other, but more so for others. Pain surprise, but not signed prediction errors, elicited anterior insula activity in both targets. These findings show that predictive coding can characterize vicarious pain, suggesting that top-down priors influence decisions on another's expected and experienced pain. Importantly, the observed prosocial biases and enhanced neural processing of risk for others highlight that uncertainty exerts a stronger influence in other-regarding decision-making compared to self-regarding choice. These findings lead to significant implications for social interactions and clinical contexts involving surrogate decision-makers.

## Introduction

Predictive coding offers a powerful framework for understanding how the brain processes sensory information, including the subjective experience of pain [1]. This model posits that the brain constantly generates predictions about incoming sensory input, and pain arises from the influence of these predictions on actual nociceptive signals, modulated by top-down factors such as beliefs and expectations[2]. While predictive coding has provided valuable insights into individual pain processing[3], a critical question remains: can this framework be extended to understand how we infer and respond to the pain of others?

Pain is not a direct readout of nociception; rather, it emerges from the integration of bottom-up nociceptive inputs with top-down processes, such as prior beliefs. Pain perception is shaped by expectations and beliefs [4], as evidenced in placebo and nocebo effects[1]. Moreover, unpredictability has been shown to amplify pain perception[5,66], underscoring the role of uncertainty, though this effect has recently been challenged in a meta-analysis[7]. Within a predictive coding framework, pain is understood to be an inferential process [8,9], wherein the brain generates predictions on what one should feel given sensory input. While pain remains subjective, computational models, in combination with neuroimaging, allow us to formally assess how pain is modulated by factors such as uncertainty, surprise, and otherness. Though uncertainty and surprise are often framed in affective terms[10], they can also be formalized within predictive coding to characterize pain beyond its raw sensory manifestation.

As social beings, individuals frequently act on behalf of others. Inferring another's pain presents a unique challenge, as it cannot be directly accessed through our own sensory systems [11]. Decisions made on behalf of someone in pain are inherently uncertain, relying on indirect cues like facial expressions, verbal reports, and our own internal models of others' states [12]. This uncertainty is further amplified by factors such as personal bias, social distance and the lack of shared physical experience [13, 14]. Understanding how we navigate this uncertainty when deciding about another's pain is crucial in various social and clinical contexts, where individuals frequently act as surrogate decision-makers for those unable to fully express their needs[14, 15].

While research has explored decision-making under uncertainty for oneself [16,17], and to a lesser extent for others in domains like monetary reward[18], the neural mechanisms underlying how we process uncertainty specifically related to another's pain remain poorly understood[19].

In monetary decision-making, uncertainty promotes risk aversion for gains and risk-seeking for losses[20]. This pattern of risk-seeking extends to the loss domain, characterized by pain or disease[21]. Further, uncertainty appears to provoke risk-seeking when deciding for others in the monetary domain [22], but this pattern does not appear to persist in the context of another's pain[23]. Given the ubiquitous but critical event of decision-making on others' pain, a process that is especially susceptible to uncertainty, it is of significant import that we gain a more fine-grained understanding of the possible factors influencing the process.
Moreover, how predictive coding principles, which have been so informative for understanding our own pain experience, apply to this vicarious context is largely unexplored. Two key studies have investigated the vicarious pain through a predictive coding framework, dissociating expected pain from uncertainty. One study found a hyperalgesic effect of uncertainty on pain assessment, indicating an independent consideration of uncertainty independent of expected intensity [24], while its recent replication shows no evidence of uncertainty's effect on pain assessment [6].

Neuroimaging studies on decision-making under uncertainty commonly implicate regions in the striatum[25–27] and anterior insula[18,28–31]. The role of these regions in processing uncertainty extends across domains[32], making them prime candidates for investigating inferential processes related to pain and self-other interactions. The anterior insula, in particular, has been repeatedly implicated in pain processing[33–37]. Investigating the similarities and differences in neural representations of pain inference for oneself and others will provide insight into whether individuals use their own experiences as a model when making decisions for others. In addition, by applying predictive coding models to neuroimaging responses to pain, we can examine the role of both expected pain and its uncertainty and how these factors influence both the experience of pain and the actions taken to address it, providing an expanded understanding of pain.

In this study, we examine how uncertainty affects pain-related decision-making for oneself and others at both behavioral and neural levels. We frame this question within a predictive coding model, formalizing inference through computational measures of expected pain, risk (as a measure of uncertainty), and errors in inference (signed and unsigned prediction errors). Participants performed a decision-making task in an fMRI scanner, where they had the opportunity to mitigate threatened pain first through a lottery, then through a wager. Uncertainty was introduced via probabilistic visual cues, allowing us to capture a

hypothesized inferential process. Trials were presented in two blocks, one targeting self-pain and the other, another's pain. We hypothesize that (1) a neural representation of another's predicted pain scales with its expected value and associated uncertainty (risk); and (2) key regions implicated in decision-making under uncertainty—particularly the striatum and anterior insula—will respond to trial-by-trial values of risk and surprise for both self and other conditions, and (3) pain prediction errors will modulate subjective pain ratings for oneself and others[38–40].

Intro word count: 865

## Results

Of the 36 participants enrolled in the study, 2 were excluded from analysis because laser fluence levels for the hand (which are lower in energy range) were erroneously used on 2 participants' ankles resulting in a lack of perceived pain. An additional participant was excluded from analysis due to a misplacement of the MR head coil, resulting in only half of the coils receiving signal. The remaining participant pool comprised 33 individuals (13 Male; average age, 23.22 years, sd = 4.33) participating in 33 dyads. Efforts were made to counterbalance DA sex when possible, alternating between males and females, but the participant pool consisted mostly of women. Twelve dyads consisted of agents of different sex across the dyad. Mean payout was 17.28 CHF (sd = 3.65). Of the 33 participants, 5 consistently made the same choice for themselves across trials; of these, 3 always gambled and 2 always selected the sure option. Two participants (one of which was also one of the 5 consistent self gambles) always selected the same option for the other (1 gambler and 1 fully risk averse). Finally, 2 participants made no bids in the self condition. All participants bid > 0 CHF for the other condition.

### Behavioral Results

*Model 1*

In model 1, we examined choice selection (a binary variable) as a function of a number of predictor variables (see methods). We found that expected values of pain (EP1) (**t = 2.23; p = 0.026**), risk (**t = 2.54; p = 0.011**) and selection for the other (**t = 2.64; p = 0.008**) predicted a sure option. Furthermore, choice response time for the other (**t = 2.33; p = 0.020**) and EP1 for the other (**t = 2.32; p = 0.020**) led to a higher frequency of sure option selection.

Model 2

In model 2, we analyzed bids made as a function of decision-making variables and targets. Here, we found that EP1 predicted higher bids (**t = 7.98, p < 0.001**) as did risk (**t = 2.96, p = 0.003**) and bid response times (**t = 12.60, p < 0.001**). In addition, choices made for others elicited marginally higher bids (**t = 1.85, p = 0.065**) especially in interaction with higher expected values of pain (**t = 3.62; p = 0.0003**).

*Model 3*

In model 3, we examined pain ratings as a function of decision variables and targets. Here we find an expected significant effect of pain outcome on rating (**t = 16.93; p < 0.001**). With

respect to target specific effects, we find a significant inflation of pain ratings predicted by the other's pain outcome (**t = 3.51; p = 0.0005**) and a positive but non-significant association between higher bids for others and higher pain ratings (**t = 1.80; p = 0.073**). Inferential errors, both signed and unsigned prediction errors (surprise), had no effect on ratings [7].

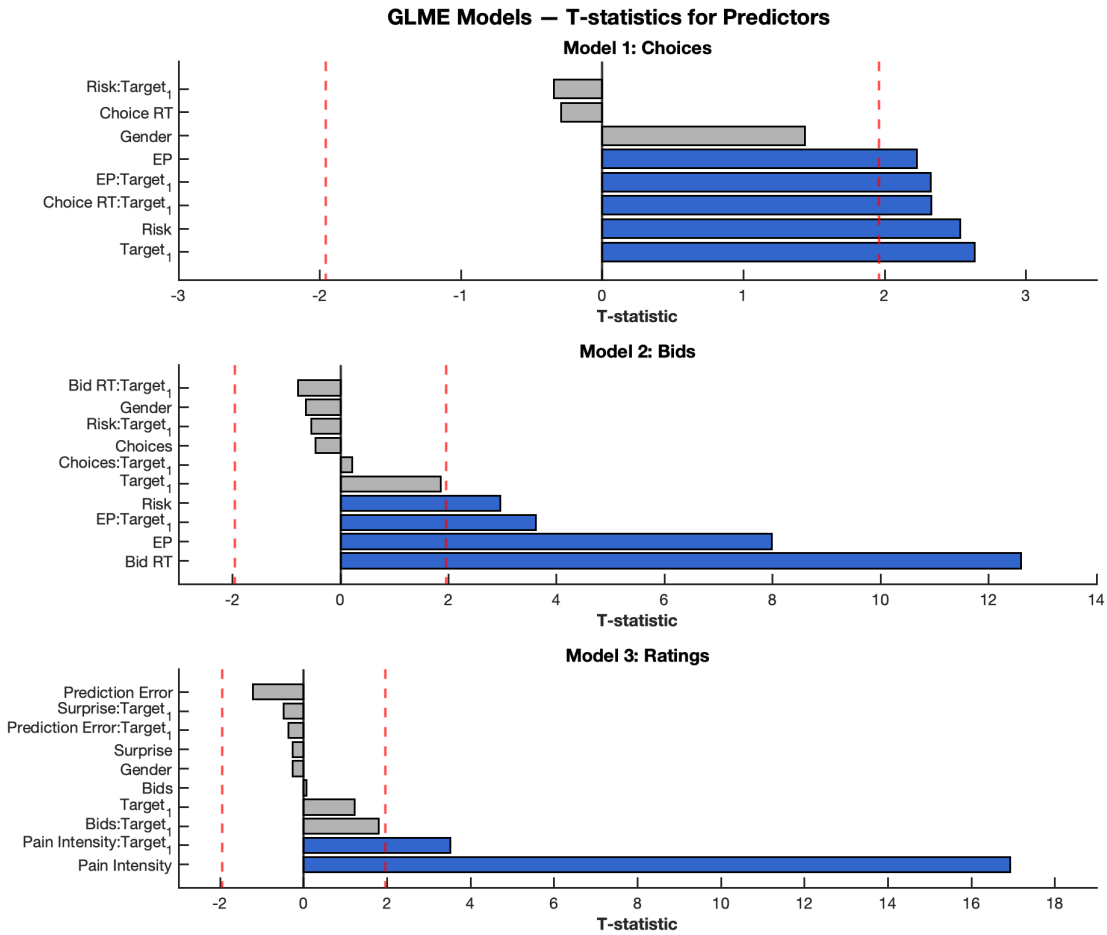


**Figure 2.** T-Statistics from Behavioral GLME Models. T-statistics for fixed-effect predictors from three generalized linear mixed-effects (GLME) models: (A) choice behavior, (B) bid value, and (C) pain intensity ratings. Each horizontal bar reflects the t-statistic for a fixed-effect term; red dashed lines mark approximate significance thresholds ($|t| > 1.96$). The x-axis is scaled dynamically to reflect the range of t-values, with the left bound fixed at –3. Choice behavior was influenced by expected pain (EP), risk target identity and reaction time. Bids varied with EP, reaction time, target and risk. Pain ratings were driven by actual outcome intensity, especially for the other, with no significant effects of prediction error terms. All models included subject-level random intercepts and controlled for gender.

Taken together, results suggest a differential pattern of choice behavior for a pain threat to another, in the form of heightened risk aversion in both models 1 and 2, higher pain relief valuation for the other in Model 2, and inflated pain ratings in model 3. A direct effect of uncertainty (risk) on decision-making was only found in the prediction phase of the decision and neither prediction errors affected subjective pain ratings.

## Neuroimaging Results

### *Voxewise Analysis*

All t-tests were performed separately for each target (Self and Other) and between each decision-target. To determine if pain inference could be identified in the brain and distinguished between self and other, we analyzed 1) expected pain and its associated uncertainty (risk) at both cue presentation ( timepoint 1, t1) and following the bid outcome (timepoint 2, t2); and 2) pain prediction error and pain surprise (risk prediction error), following pain delivery outcomes. In addition, to confirm the validity of our design, we tested for pain intensity at trial outcome (BOLD onset modulated by pain intensity level).

### Contrast: Expected Values and Risk

Expected values of pain for the other elicited positive responses in the right cuneus, left and right fusiform gyri, left middle occipital gyrus and left mid-cingulate gyrus, while no significant responses were found for one's own expected pain. However, one's own expected pain negatively correlated with significant responses in the right medial oribital gyrus, extending into the anterior cingulate and the right angular gyrus. When testing expected values of pain responses against each other for self and other, we find a significant response in the left fusiform gyrus.

When examining risk responses separately for each target, we find no significant responses for the self condition, but widespread responses for the other, including in key areas of uncertainty processing, the cingulate cortex and the putamen, as well as other regions in frontal, occiptal and temporal areas. A direct comparison between self and other risk computation yields significant responses in the right middle temporal gyrus for other > self risk.

## Figure 3: Predictive Phase Neural Correlates

### (a) Expected Pain, Other

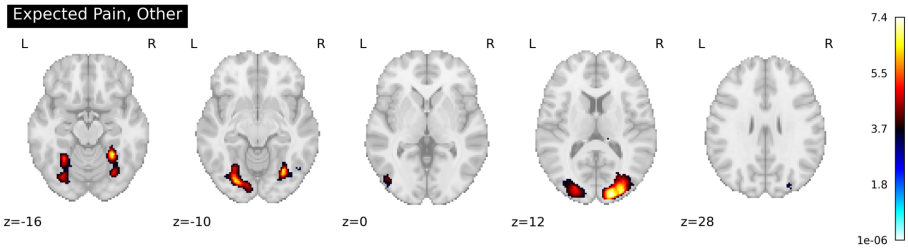


### (b) Expected Pain, Negative, Self

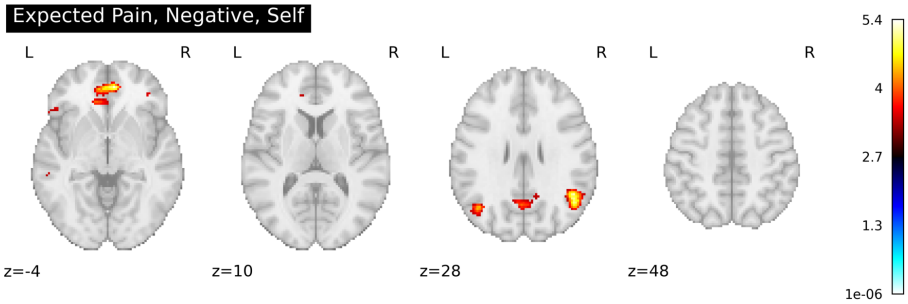


### (c) Risk, Other

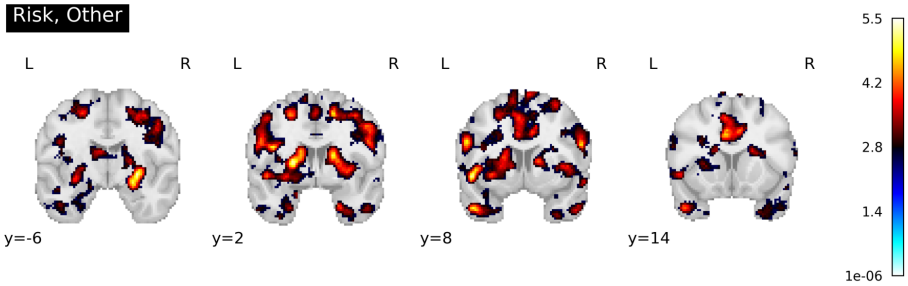


### (d) Risk, Self

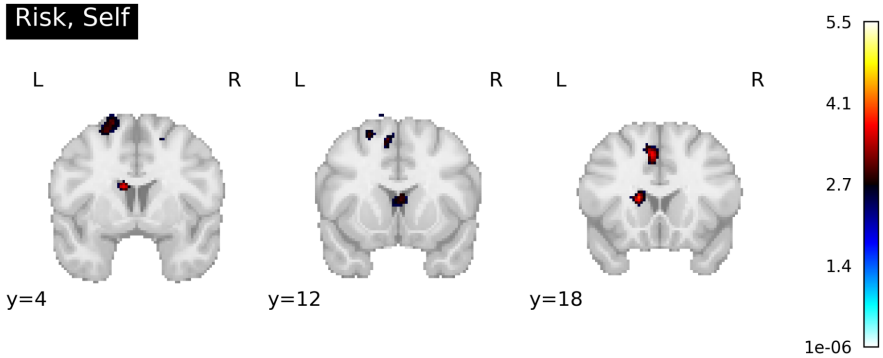


### (e) Risk Self < Risk Other

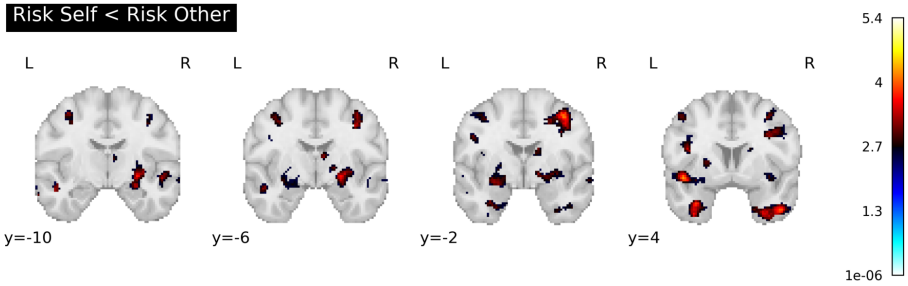


1

**Figure 3: Neural Correlates of Expected Pain and Risk (Predictive Phase)** Thresholded t-statistic maps of the BOLD response for expected pain and risk during the predictive phase. **(a) Expected Pain, Other:** Axial slices (z = -16, -10, 0, 12, 28 mm) showing positive responses to expected pain for the other, primarily in visual and cingulate cortices. **(b) Expected Pain, Negative, Self:** Axial slices (z = -4, 10, 28, 48 mm) showing negative correlations with one's own expected pain in the right medial orbital gyrus and right angular gyrus. **(c) Risk, Other:** Coronal slices (y = -6, 2, 8, 14 mm) highlighting significant responses to risk for the other, including bilateral caudate, putamen, and anterior insula. **(d) Risk, Self:** Coronal slices (y = 4, 12, 18 mm) highlighting significant responses to risk for the self, primarily in the left caudate. **(e) Risk Self < Risk Other:** Coronal slices (y = -10, -6, -2, 4 mm) showing significant differential responses in the left anterior insula and right putamen. Whole-brain maps (a, b, c) were thresholded at $p<0.001$ (uncorrected) and cluster-corrected at $k=25$ voxels ($p<0.05$ FWE). SVC analyses (d, e, f) were conducted with a starting voxel threshold of $p=0.01$ and corrected at $p<0.05$ FWE. Color bars indicate t-statistic values.

Contrast: Pain, Pain Prediction Error and Surprise

The neural response to pain outcomes yielded a widespread network whose activity was positive linearly coupled with the intensity of the stimulation in the self. This included the bilateral anterior insula, extending to the posterior insula; and bilateral thalamus; the middle cingulate cortex; left postcentral gyrus; left superior parietal lobule; and putamen as well as the right superior frontal gyrus and parietal operculum.

In the other condition, we found no significant responses to pain intensity at the whole brain level.

Inferential errors (both signed pain prediction error and surprise) yielded no significant responses, except for surprise in the self condition, associated with a significant response in the right postcentral gyrus.

*ROI Analysis*

An ROI analysis was performed on expected values of pain, associated risk, as well as on pain, pain prediction error and pain surprise, for each target separately, and contrasted between targets. We focused on regions commonly implicated in inference and uncertainty, namely the anterior insula; and dorsal striatum (caudate and putamen).

## Figure 4: Post-Outcome Phase Neural Correlates

### (a) Pain, Other

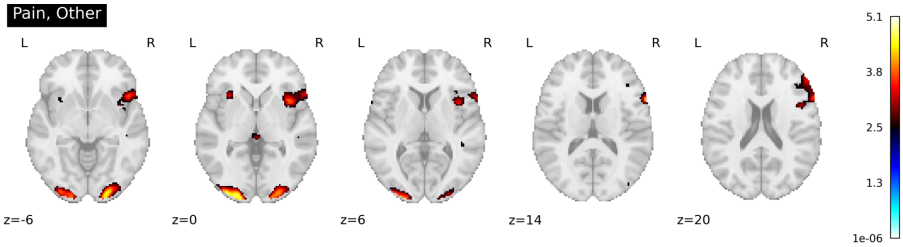


### (b) Pain, Self

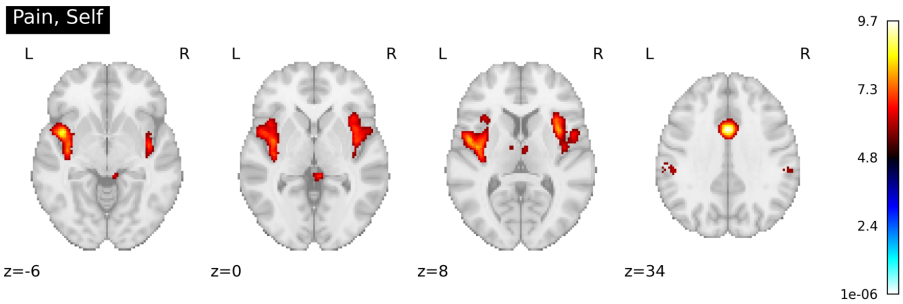


### (c) Pain, Other, Negative

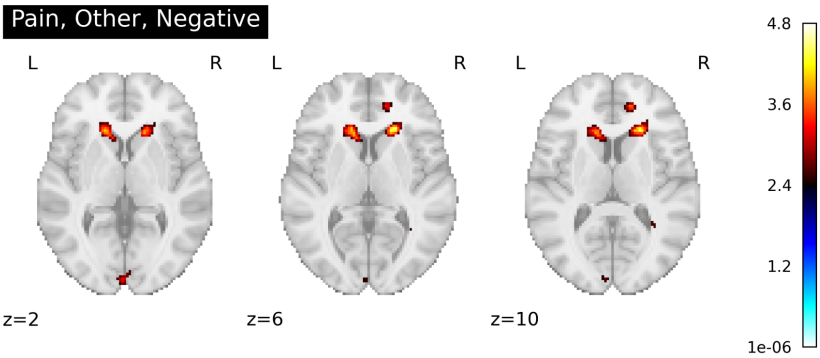


### (d) Pain Surprise, Self

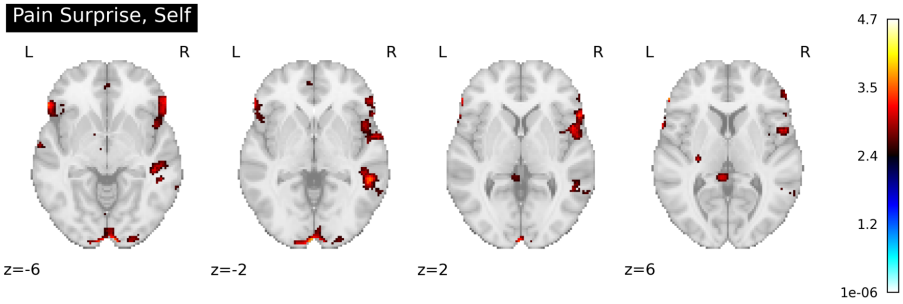


### (e) Pain Surprise, Other

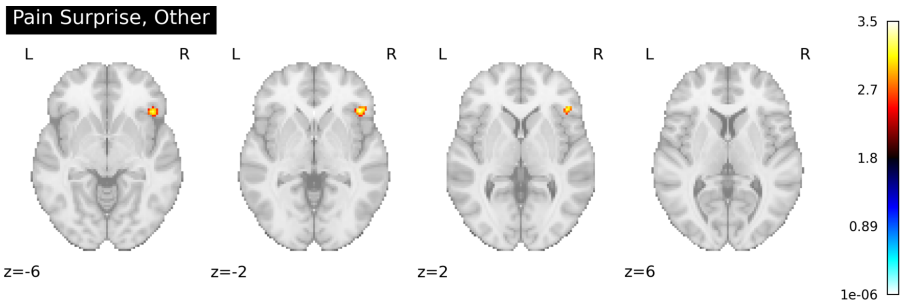


1

**Figure 4: Neural Correlates of Pain Intensity and Surprise (Post-Outcome Phase)**Thresholded t-statistic maps of the BOLD response for pain intensity and surprise at trial outcome. **(a) Pain, Other:** Axial slices (z = -6, 0, 6, 14, 20 mm) showing activity in the right anterior insula and negative association with the caudate. **(b) Pain, Self:** Axial slices (z = -6, 0, 8, 34 mm) showing widespread activity in response to self-pain intensity, including bilateral anterior insula, thalamus, and middle cingulate cortex. **(c) Pain, Other, Negative:** Axial slices (z = 2, 6, 10 mm) showing negative correlations with other's pain in the bilateral caudate. **(d) Pain Surprise, Self:** Axial slices (z = -6, -2, 2, 6 mm) highlighting activity in the right anterior insula, consistent with 'Pain Surprise, Other'. **(e) Pain Surprise, Other:** Axial slices (z = -6, -2, 2, 6 mm) highlighting activity in the right anterior insula. Whole-brain maps (a, b, c) were thresholded at $p<0.001$ (uncorrected) and cluster-corrected at k=20 or k=25 voxels ($p<0.05$ FWE, as specified in text/tables). SVC analyses (d, e) were conducted with a starting voxel threshold of $p=0.01$ and corrected at $p<0.05$ FWE. Color bars indicate t-statistic values.

Contrast: Expected Values and Risk

Expected values of pain in the other versus the self showed a significant response in the left caudate. Pain risk evoked significant responses in the left caudate in both targets. Pain risk for the other elicited responses bilaterally in the caudate, putamen and anterior insula. When comparing self vs other pain risk, we find a significant response in the left anterior insula and right putamen.

Contrast: Pain, Pain Prediction Error and Surprise

Another's pain incurred a response in the right anterior insula and a negative association with the caudate bilaterally. Finally, surprise elicited a significant response in the right anterior insula for both the the self, as well as for the other.

## Discussion

Predictive coding accounts of pain have garnered significant interest recently [41–44]. Our study builds on this framework, investigating the neural underpinnings of decisions made regarding another's pain, a process inherently laden with uncertainty. Our findings broadly support our hypothesis that the brain encodes vicarious pain components within a predictive coding framework, mirroring self-pain mechanisms in certain aspects while showing unique modulations for others. Specifically, our findings reveal 1) a graded neural representation of predicted other-pain, distinct from self-pain; 2) implicate the dorsal striatum in processing pain uncertainty (risk) and more strongly for others; and 3) show anterior insula involvement in pain surprise for both self and other. Our results therefore support hypotheses 1 and 2. Hypothesis 3 however was not supported: while evidence of unsigned prediction errors emerged in the brain, they did not impact subjective pain ratings in either self or other. These results support the application of predictive coding to vicarious pain processing, highlighting the brain's capacity for graded computations absent direct nociceptive input. Further, we replicate previous results at the behavioral level showing increased risk aversion and pain

relief valuation when deciding for others, as well as an overestimation of delivered pain. We do not replicate an effect of uncertainty on pain evaluation however.

Risky decision-making for others' pain

Behavioral results on decision-making for others' pain largely align with our previous findings[19], replicating a risk-averse pattern where participants were less inclined to gamble on others' pain, a result that contrasts with some reports of equal or increased risk-taking in other-regarding monetary decisions[22]. Consistent with our earlier work, we also observed a higher monetary valuation of others' pain relief compared to one's own and an overestimation of others' pain intensity, suggesting a cautious and potentially error-minimizing approach to vicarious pain evaluation, diverging from documented underestimation by clinicians [45–47]. Reaction time data further indicated increased deliberation for others' decisions, a hallmark of higher uncertainty [48]. More risk-averse, costlier decisions in conjunction with inflated pain ratings may point to altruistic motivations as has previously been found in other studies[49–51] but we stress two caveats to this observed behavior: first, agents, including in our study, may be complying with an implicit experimenter demand or social norm; second, individuals may be attempting to compensate for uncertainty rather than diminish another's pain; third, individuals may well be altruistic in a one-on-one scenario, where they alone incur the responsibility of another's pain, and therefore cannot diffuse accountability or guilt across, for instance a group[52–54]. We speculate that observed other-regarding choice behaviors belie a drive to minimize for the uncertainty stemming from a disembodiment of the agent relative to the target. In our previous study, we further found that uncertainty (risk) dampened the estimation of another's pain. We do not replicate this finding in our current study and speculate that this null result may be a consequence of occlusion and physical social distance between members of the dyad. In the first study, dyads were seated at the same table during the experiment, witnessing their confederate's experience, while dyads in the current study were relegated to separate rooms and could not see or hear eachother otherwise. These differences in experimental set-up may explain a lack of effect of uncertainty on pain estimation. Taken together, behavioral differences between self and other decisions suggest different weighting schemes for similar internal models when processing vicarious pain.

Mental representation of expected pain and its risk, in self and other

Pain is modulated by belief[55–57]. From a predictive coding perspective, pain anticipation should involve a mental representation of the expected stimulus and its associated uncertainty. Our findings of significant positive neural responses to trial-by-trial expected pain for the other in visual areas (occipital and fusiform gyri), the cuneus and the cingulate, implicated in both own and vicarious pain[58] provide novel support for hypothesis 1, demonstrating a graded neural representation of predicted vicarious pain. The visual cortex activation might reflect increased attentional processing of cues related to the other's potential pain [59,60], while mid-cingulate involvement could indicate a predictive modeling of the anticipated sensory consequences for the other[6162]. Interestingly, we did not observe a similar positive neural response to one's own expected pain. Instead, we found significant negative responses in the orbitofrontal cortex, a key area in valuation[63], extending in the anterior cingulate, a region implicated in decision-making, anticipated negative outcomes [64] and opting for pain avoidance[65]. This asymmetry may suggest a differential framing of self-versus-other pain in terms of (negative) reward. We speculate based on this result that individuals may apply a different frame in pain decision-making for themselves and others, where other-regarding scenarios pit pain as punishment, and no-pain as zero; but self-regarding reference frames place pain as zero and no pain as reward[66].

Mental representations of expected pain risk, in self and other

In further support of predictive coding's explanatory power in pain inference, we find significant neural responses to pain risk decoupled from pain expectation, in several visual and frontal areas between pain targets. Risk computation for another correlates with significant responses in the cingulate cortex, a region previously found to process vicarious predicted reward[67] and that is consistently implicated in uncertainty processing[68–70], and the dorsal striatum, recently highlighted as the most reliable region in test-retest studies on decision-making under risk[71]. Consistent with our behavioral findings of increased risk aversion for others, we observed a comparatively enhanced neural response to pain risk when considering the other. This stronger striatal engagement for other-risk, supporting hypothesis 2 regarding the role of the striatum in uncertainty, may reflect a compensatory mechanism to address the heightened uncertainty inherent in inferring another's internal state.The self-other distance may increase the weight of potential negative outcomes, demanding more robust neural processing of risk. In our ROI analysis, the dorsal striatum showed significant

responses to pain risk for both self and other. However, the anterior insula exhibited a significant response to *other*-risk that was not found in self-risk. The dorsal striatum and anterior insula are expecteded to respond to risk for both targets; here we find only partial evidence of a common neural grounding, suggesting increased risk processing for the other, relative to one self, rather than spatially distinct risk processing for self vs other, a nuance that warrants further investigation. Overall, these findings support the notion that individuals employ similar computational models to track both expected pain and its associated uncertainty for themselves and others, in support of predictive coding's generalizability and applicability to pain prediction[1,33], albeit with notable differences in the intensity and potentially the specific neural substrates involved.

Pain, prediction and error

Having established the plausibility of a predictive coding mechanism in inferring both one's own and another's pain, we now turn to the role of inferential errors. Notably, across both self and other targets, pain surprise (the unsigned prediction error) evoked activity in the right anterior insula, a finding consistent with prior research implicating this region in processing surprise across various cognitive domains[32] and pain inference [33,72–75,76]. This involvement of the anterior insula in surprise for both self and other supports hypothesis 2 regarding its role in processing violations of expectation. Importantly, surprise responses for both self and other were evoked in the same constrained region previously reported for both perceptual and economic surprise, in further support of common computational mechanism deployed in the anterior insula across functions and contexts. We did not, however, find a significant neural response to signed prediction error, either in self or other.

One perspective within predictive coding is that pain itself can be viewed as both a prediction (of potential tissue damage) and a prediction error (signaling a deviation from an expected, non-painful state). Given the anterior insula's prominence in both pain processing and error signaling, it's possible that neural responses to the raw pain signal in this and related regions might, to some extent, encompass the processing of signed and unsigned prediction errors. More generally, recasting pain as both prediction and prediction error within an interoceptive framework[3,77] offers an additional means by which to characterize pain in empirical and theoretical settings in future studies.

## Applications and Implications

Our results yield several implications. First, we identify costly pro-social tendencies when individuals are faced with another person's pain. This pro-sociality may be motivated by a desire to attenuate pain in another[78]; or decrease uncertainty in inferring another's state[23]; or to conform to a social norm (politeness)[79] under third-party observation[80]. Whatever the motivation, costly pro-sociality clearly wins over selfish concerns. Further, these results show distinct processes for decision-making on pain for self and other, suggesting that between simulation and theory-theory[81], we treat others differently than we do ourselves. However, we also find commonalities in processing our own and others' pain, specifically when examining second-order inferential parameters, namely risk in the predictive phase, and surprise in the error. In both targets, risk computation elicits a dorsal striatal response; and surprise, an anterior insula response, supporting a common mechanism applied to both targets' inferential processes. Beyond informing surrogate decision-making, these findings offer critical insights for clinical pain management, where others' pain is, in contrast to our results, often underestimated. By elucidating how caregivers' expectations and uncertainty about patient pain can influence their perception and treatment choices, further precision in pain assessment, perhaps informed by artifical intelligence, may resolve the gap between perceived versus experienced pain.

## Limitations

The study is not without limitations, including a comparatively low sample size given the low number of trials for each participant. The low number of trials was linked to the willingness-to-pay event in each trial, which should not be repeated[82]. A future study can eliminate this step, allowing for more trials to be conducted in a scanning session. In addition, in our study, agents do not observe the other during the decision-making process and therefore base their choices on numbers displayed and their prior beliefs. They do not employ such cues as targets' facial expressions[83], vocalizations[84] or declarations[85], unlike our previous study, where agent and target were seated next to each other and therefore conveyed additional information to the decision-maker. This difference in context may prove critical to further studying the effects of uncertainty on perceived pain in others. At the same time, as decisions made in our study were blind and disembodied they can be simulated by an artificial agent that, in the future, may provide guidance on clinical decision-making in pain given

established statistical parameters (probability of pain, expected pain risk and unexpected pain outcomes).

Conclusions

In this study, we provide compelling evidence for a neurally instantiated, graded representation of another's expected pain, demonstrating an intrinsic, computational mechanism for vicarious pain processing that integrates both the likelihood and magnitude of potential harm. By applying a predictive coding framework and employing model-based fMRI, we have illuminated the critical role of uncertainty – from prediction to experience and assessment – in shaping how we perceive and respond to the pain of others, offering a direct comparison with our own pain processing. Our findings reveal both shared and distinct neural substrates underlying self and other pain decisions, notably highlighting the graded representation of vicarious pain prediction and the representation of unexpected pain outcomes (surprise) on neural responses. While neural responses to pain prediction errors were observed, these errors did not significantly impact subjective pain ratings for either oneself or the other. Ultimately, this work expands the applicability of predictive coding to the domain of social cognition, providing a novel computational and neural account of how we navigate the inherent uncertainty of others' suffering, with significant implications for understanding empathy, social behavior, and the development of more human-centered approaches in clinical and artificial intelligence contexts.

Discussion Word Count to date: 1930

## Methods

Population

The study was conducted at the Campus Biotech in Geneva, Switzerland. A total of 36 participants enrolled in the study. Participants were recruited from both the University of Geneva Campus and the general population. Inclusion criteria included: French-speaking; 18 -45 years of age; and good general health. Exclusion criteria included: reported psychiatric or neurological diagnoses; current or recent psychotropic drug use; claustrophobia; metal or other implants that may interfere with the MR scanner. Study information, including the task procedure and MR safety guidelines, was sent electronically to all participants 2 days before the scheduled experiment session. Upon arrival at the study center, participants were given

paper versions of the information and consent forms. Participants were asked to read these, confirm their understanding of the study's risks and benefits, and sign the forms before continuing with the experiment. Following intake, the experimenter verbally explained the study structure and task process. Once participants understood the experiment, they were each assigned a fixed role in the task: they were either cast as a Deciding Agent (DA), or a Passive Recipient (PR). The DA's role in the experiment was to enter the scanner, and make decisions both for herself and the PR. The PR's role was to act as the recipient of half of the DA's decisions. The study was approved the Commission Cantonal d'Ethique de la Recherche sur L'Etre Humain in December, 2019. Data collection was conducted between April and July, 2021.

## Procedure

Following intake, both participants were asked to remove metallic items and leave personal affairs in dedicated lockers before being led to the scanner control room. Here, both participants were briefly shown the laser pain stimulation machine and the PR was asked to take a seat in the control room. As the study occurred during the COVID19 pandemic, all participants and personnel were wearing masks but the DA was asked to remove her mask before entering the MR room and being settled into the bore. Once in the scanner room, they were given earplugs and MR compatible headphones. Several sensors were fitted on the DA, including a pulsemeter to record cardiac signals; a pneumatic sensor around the waist to measure respiration; and two electrodes on 2 of the left-hand fingers, to record skin conductance. Before placing the coil, DAs were shown the button response box on which they were to provide their answers. They were then moved into the scanner to begin image acquisition. Finally, a laser-safe cloth was draped over the opening of the bore, to ensure that, in case a laser emission went astray, it would not harm the participant.

While DAs were entered into the scanner, they were led to believe that PRs were undergoing a pain calibration procedure in the control room. In reality, no such procedure was performed. For security reasons, a deception was introduced to the study, whereby the DA was led to believe the PR would be the target of the pain on half the task trials, requiring an initial pain calibration procedure. This deception was included in the study because the MR scanner control room in the Campus Biotech does not conform to safety requirements for laser emission. Therefore, after settling the DAs into the scanner and launching a first MR sequence (localizer), PRs were paid 30 CHF, debriefed, and sent home.

## MRI acquisition

Scans were acquired in a 3T Siemens MRI scanner located at the Campus Biotech MRI platform. Sequences during the study were acquired as follows: a field-map scan (2D GR TR=677ms/TE=4.92ms/FA=60deg/SO=PFP); two functional scans of about 20 mins each ([112 112 72], 2D EP TR=1100ms/TE=32ms/FA=50deg, Mosaic Multi-band) where the task was administered; a T1-weighted anatomical scan ( [256 256 208], 3D GR\IR TR=2200ms/TE=2.96ms/FA=9deg/SO=IR\PFP).

## Pain Calibration Procedure

The experimental task required 3 levels of pain (low, medium and high) to be made available to the decision target. Because pain is a subjective experience, we performed a calibration procedure on the DA, following her field map scan acquisition and prior to starting the task. This calibration procedure consisted of stimulating the area around the DA's ankle bone, as this body part was 1) accessible to the experimenter; 2) glabrous skin. Pain stimulations were evoked via nociceptive radiant heat stimulation using an infrared neddymium: yttrium-aluminium-perovskite laser system (Nd: YAP; Stimuli 1340; El. En, Florence; lambda = 1340 nm; pulse duration, 4 ms; beam diameter 6 $mm^2$). The wand of the laser stimulation was passed through an opening in the wall separating control and MR rooms to allow the experimenter to administer stimulations on the DA during functional scans. Stimulations at energies of 1.5-3 J were emitted randomly in step intervals of 0.25 J, three times each. After each stimulation, DAs rated the pain experienced on a scale presented on the in-bore screen using the button response box. The scale ranged from 0 to 10, with 0 indicating no pain, and 1 a first pain, consistent with our previous research[23]. Responses for each energy level were then averaged such as to obtain a low, medium and high pain level (average ratings closest to 1; 5 and 9, respectively). In cases where a pain level was equal to another, an additional 0.25 J was added to the higher pain level. Once individual pain levels were computed, the 3 pain levels were presented to the DA once more, to ensure the participant knew which pain corresponded to her assignation of low, medium and high levels. During the calibration and the task, all parties present were required to wear laser safety goggles. The only exception was the DA whose upper half of the body was protected by laser-safe curtains certified for the wavelength of the stimulator.

Task procedure

DAs performed two blocks of 18 trials of a decision-making task in the scanner. At each block, participants started off with an endowment of 216 monetary units (MUs), equivalent to 21.6 CHF. At each trial, DAs were first presented with a visual cue, depicting a probability (in the form of a red pie chart on a grey background), and an intensity (represented by 2 or 3 red lightning bolts) of threatened pain, for 6 seconds. Probabilities ranged from 0.1-0.9 in steps of 0.1. DAs were then given 6 seconds to either gamble to avoid the pain altogether, with a 50% chance of winning; or select a sure option, where, if pain were the outcome, it would certainly be reduced by one level. Participants that did not respond in time incurred a penalty of 10 MUs. In the next screen, participants were asked to bid on their decision, selecting a price that ranged from 0-10 MUs on a scale. Participants that did not respond in the allotted 6 s entered a default "0" for their bid. DA bids were then compared to a hidden reserve price randomly selected for each trial. Bids matching or exceeding this reserve price were accepted as purchase prices for the initial decisions, and the latter were applied to initial values of expected pain, while rejected bids left the DA facing the initial probability and intensity of threatened pain. The bid status (accepted or rejected) was presented on the screen for 6 seconds. Finally, pain was delivered depending on resultant probabilities and intensities. A visual cue representing this pain delivery was simultaneously presented on the in-bore screen, as either initial values of pain intensity (2 or 3 red lightning bolts); reduced values of pain intensity (2 or 3 yellow lightning bolts) or no pain (3 greyed out lightning bolts). In no pain trials, DAs received a non-painful laser stimulation of 0.5 J. The outcome screen was presented for 6 seconds. Finally, DAs were asked to rate the pain outcome on a visual rating scale, this time anchored by two emojis, one happy and the other unhappy. The scale ranged from 0 to 10, with 0 replaced by the happy emoji. Trials were jittered by an inter-trial interval selected from a 2-5 s range, during which a black fixation cross on a grey screen was presented. DAs played one block where the decision target was the PR; and another where it was themselves. Block order was randomized across participants, as were buttons assigned to gambles or choices (left and right, to avoid lateralization effects) and placement of happy/unhappy emojis (left/right). Pain was genuinely administered to the DA during DA target blocks, but no actual pain was delivered during PR-target blocks.

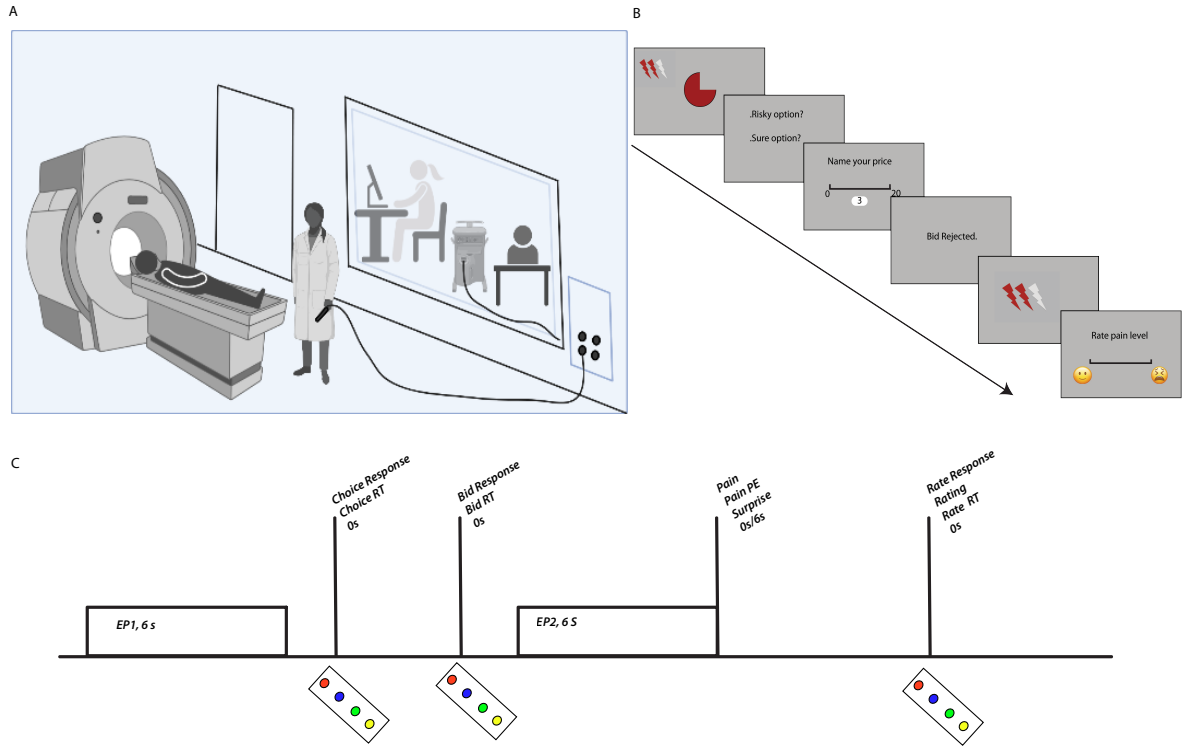


**Figure 1.** A) Experimental setup. Deciding agents made decisions on threatened pain for themselves and others during an fMRI session. An experimenter delivered pain via laser within the scanner room. The participant was made to believe the other remained in the control room and was subject to pain delivery during the "Other" block condition. B) Sample Trial. Participants were first shown a visual cue representing an initial value of expected pain with the probability of delivery exhibited in a pie chart, and pain intensity by red lightning bolts. They were then asked to 1) either gamble to avoid pain or; 2) choose a sure option to reduce pain. They were then asked to place a monetary bid on their choice, which was then compared to a hidden, randomly generated reserve price. The participant was then told whether the bid was accepted or not, and the pain outcome was subsequently shown or delivered based on the expected value of the threatened pain following bid outcome. Participants were then asked to rate the perceived pain, for themselves in the "Self" condition, or the other felt in the related condition. C) fMRI Design. The general linear model constructed for fMRI analysis included, 1) cue onsets, parametric modulated for expected value and risk; 2) Choice onsets, modulated by choice response time; Bid onsets, modulated by bid RT; 3) Bid outcome modulated by expected value and risk; 4) Pain outcome, modulated by pain intensity, signed pain prediction error and surprise; 5) Rating onset, modulated by rating response time.

Prior to performing the tasks, DAs played 3 practice rounds of the task, with the experimenter guiding them through each screen over the microphone. Only once participants confirmed their understanding of the task did the latter commence. Further, each block began with task instructions presented onscreen. Participants could begin the task when ready, by pressing a button. At the end of the two experimental runs, one payout of the blocks was randomly selected as payment (rounded down or up to the nearest integer) in addition to time paid for participating (50 CHF). Finally, we acquired the T1-MPRAGE anatomical scan, before

removing the DA from the scanner. Once out of the scanner, the DA filled out a short series of questionnaires, before being paid, debriefed and sent home.

## Computational Models

To capture the underlying inference hypothesized in this paper, we apply computational models of decision-making under uncertainty to characterize neural processes related to presented stimuli and outcome; and to explain observed behavioral choices. We employ pre-existing models testing the effect of uncertainty on economic decision-making[86], adapted to the domain of pain assessment and treatment.

## Computational Model Equations

We employed computational models to quantify key variables related to decision-making under pain uncertainty. These variables were calculated on a trial-by-trial basis.

**Expected Pain at Cue Presentation ($EP_1$)** At the initial cue presentation, the expected pain ($EP_1$) represents the average pain intensity given the probabilities of the outcomes. Assuming one outcome is a potential pain intensity $P$, with probability $p_1$, and the other outcome is no pain (intensity 0):

$$EP_1 = p_1 \cdot P + (1 - p_1) \cdot 0$$

$$EP_1 = p_1 \cdot P$$

Where:

- $P$: The threatened pain stimulation intensity (e.g., 2 or 3 lightning bolts).
- $p_1$: The initial probability of experiencing pain P (from the visual pie chart).

**Initial Risk ($\sigma_1^2$)** Initial risk ($\sigma_1^2$) quantifies the uncertainty (variance) associated with the expected pain at cue presentation. Given the same two outcomes ($P$ with probability $p_1$, and 0 with probability $1-p_1$), the variance is calculated as:

$$\sigma_1^2 = p_1 \cdot P^2 - (EP_1)^2$$

This simplifies to:

$$\sigma_1^2 = p_1 \cdot P^2 - (p1 \cdot P)^2$$

$$\sigma_1^2 = p_1 \cdot P^2 - p12 \cdot P^2$$

$$\sigma_1^2 = p_1 \cdot P^2 (1 - p_1)$$

**Expected Pain After Bid Outcome ($EP_2$)** Following the bid outcome, the expected pain ($EP_2$) is updated based on the participant's choice (gamble or sure option) and whether the bid was accepted.

**If the gamble option was chosen and the bid was accepted:** The probability of pain is halved (to $p_1/2$), and the other outcome remains 0.

$$EP_2 = p_1/2 \cdot P + (1 - p_1/2) \cdot 0$$

$$EP_2 = p_1/2 \cdot P$$

**If the sure option was chosen and the bid was accepted:** The pain intensity is reduced by one level ($P - 1$), and the probability of this reduced pain remains $p_1$. The other outcome remains 0.

$$EP_2 = p_1 \cdot (P - 1) + (1 - p_1) \cdot 0$$

$$EP_2 = p_1 \cdot (P - 1)$$

**If the bid was rejected (for either gamble or sure choice):** The expected pain remains the initial $EP_1$.

$$EP_2 = EP_1$$

**Risk After Bid Outcome ($\sigma_2^2$)** Risk ($\sigma_2^2$) is updated similarly based on the bid outcome and choice.

**If the gamble option was chosen and the bid was accepted:** The variance is calculated with the new probability $p_1/2$ and pain intensity P.

$$\sigma_2^2 = p_1/2 \cdot P^2 (1 - p_1/2)$$

**If the sure option was chosen and the bid was accepted:** The variance is calculated with the original probability $p_1$ and the reduced pain intensity ($P-1$).

$$\sigma_2^2 = p_1 \cdot (P-1)^2 (1-p_1)$$

**If the bid was rejected (for either gamble or sure choice):** The risk remains the initial $\sigma_1^2$.

$$\sigma_2^2 = \sigma_1^2$$

**Pain Outcome ($P_o$)** $P_o$ is the actual pain experienced or witnessed at the trial outcome.

**Signed Pain Prediction Error ($\delta_{pain}$)** Following the delivery of pain, the signed pain prediction error ($\delta_{pain}$) is the difference between the observed pain outcome and the updated expected pain:

$$\delta_{pain} = P_o - EP_2$$

**Risk Prediction used as "Surprise" :** The risk prediction error, referred to as "Surprise" throughout the study, quantifies the deviation of the squared signed prediction error from the expected variance after the bid outcome. This is an unsigned error, reflecting the unexpectedness of the outcome's magnitude relative to the updated uncertainty[86].

$$Surprise = (\delta_{pain})^2 - \sigma_2^2$$

Data Analysis

*Behavioral*

Behavioral data analyisis was performed using Matlab 2014b. We analyzed overt, behavioral responses as a function of decision-making variables listed above; and decision targets. We first modelled participants behavioral responses at the level of 1) choice; 2) bids and 3) ratings. We constructed a linear mixed model under the binomial distribution, casting choice (0 = gamble, 1 = sure option) as a function of $EP_1$, $Risk_1$, and choice reaction time (RT), as well as their interactions with the target (Self or Other). In the second, we constructed a general linear model casting bids as a function of $EP_1$, $Risk_1$, choice, and bid RT, as well as

their interactions with the target. In the third, we constructed a general linear model casting pain rating as a function of pain, pain prediction error, pain surprise, and rating RT, as well as their interactions with the target. In all models, gender was specified as a nuisance fixed factor, and partipants' identifier as a random factor (see Table 1). These models can capture how covert computations relating to uncertainty (expected pain values, pain risk, pain prediction error and pain surprise) may affect overt behavior, and distinguish potential differences in their effects on the target.

**Table 1: Description of Generalized Linear Models for Behavioral Responses** This table outlines the structure of the three generalized linear mixed-effects (GLME) models used to analyze participants' behavioral responses. Each model specifies the outcome variable, primary predictor variables, nuisance variables (fixed factors), and random effects (participant-level intercepts).

| Model | Outcome Variable | Predictor Variables | Nuisance Variables | Random Effects |
|---|---|---|---|---|
| Model 1 (binomial) | Choice | $EP_1$, $Risk_1$, Target, | Sex | Participant |
| Model 2 | Bid | $EP_1$, $Risk_1$, bid RT, choice, Target | Sex | Participant |
| Model 3 | Rating | Pain, Pain PE, Pain Surprise, choice, bids, rate RT, Target | Sex | Participant |

*Neuroimaging analysis*

Neuroimaging preprocessing and analysis was performed using SPM12. The main goal of the neuroimaging analysis was to apply a model-based approach to BOLD responses at specific timepoints of the trial that do not require an overt response from the participant. We first describe the preprocessing pipeline applied to the functional MR datasets below.

*Preprocessing*

Functional MR volumes were first converted to nifti format from dicom. Images were then slice-time corrected to the middle slice (36). Voxel displacement maps were then applied to the images, before the latter were realigned and unwarped according to head motion parameters (6; 3 translational and 3 rotational). Individual T1w anatomical volumes were then co-registered to the mean functional images and segmented according to six-class tissue probability maps (TPMs). The resulting parameters (forward deformations) were then applied

to functional volumes, which were then normalized to the standard MNI152 template, before being smoothed to a FWHM of 8 mm. The resulting preprocessed images were used for analysis.

*Voxelwise analysis*

In a first instance, we constructed a general linear model including the following onsets: cue presentation (0s); choice response (0s); bid response (0s); bid outcome (0s); trial outcome (0s for self, and 6s for other, respectively); and rating response (0s). These onsets were convolved with the canonical hemodynamic response function and parametrically modulated by the expected value and risk following choice; choice RT; the expected value and risk following bids; bid RT; pain level, pain prediction error (signed PE) and pain surprise (unsigned PE) following trial outcome; and rating and rating RT following pain evaluation. All parametric modulators were serially orthogonalized relative to one another. In addition, we included 24 noise regressors comprised of the 6 motion parameters and 18 cardiac and respiratory regressors (TAPAS toolbox). We employed the FAST algorithm to control for auto-correlation. The general linear model was performed on individual subject timeseries first, before pooling resulting contrasts of interest in a second-level, random-effects model to test group-level responses. Group analyses effects were considered significant if exceeding a threshold corresponding to $p < 0.05$ FWE corrected for multiple comparisons at the cluster level, with an underlying voxel-based threshold corresponding to $p < 0.001$ (uncorrected)[87] . Contrasts of interest focused on the following elements of the computational model, split into predictive and trial outcome phases. In the predictive phase, we tested for expected value of pain and pain risk (concatenating regressors from onsets at cue presentation and following bid outcome). In the trial outcome phase, we tested for pain intensity, signed prediction error and pain surprise (unsigned prediction error).

*ROI analysis*

To complement the mass univariate approach at the whole brain level, we selected 3 brain regions involved in inferential processes: the anterior insula; caudate and putamen (dorsal striatum). In addition, for surprise contrasts, we used ROIs centered on previously published peak BOLD responses for surprise in perceptual and valued-based decision-making[32]. Within these ROIs, results were considered significant if exceeding $p < 0.05$ FWE small volume correction at the voxel level, with a starting threshold of $p = 0.01$.

1

2 Tables

3 **Table 3: Whole-Brain Neural Correlates of Predictive Phase Variables** This table presents significant
4 clusters of BOLD activity for expected pain and risk during the predictive phase of the task (cue presentation
5 and bid outcome). Results are from a whole-brain random-effects analysis, thresholded at a voxel-level p<0.001
6 (uncorrected) and cluster-corrected at p<0.05 FWE, with a minimum cluster size (k) of 25 voxels. Anatomical
7 labels are derived from the AAL atlas.

| **Whole Brain, p = 0.001, k = 25** | | | | | | | |
|---|---|---|---|---|---|---|---|
| **EP Other** | | | | | | | |
| cluster | cluster | peak | peak | | | | Region |
| p(FWE-corr) | size | p(FWE-corr) | T | x | y | z {mm} | |
| 0 | 1263 | 0.002 | 7.37 | 18 | -96 | 12 | Right cuneus |
| 0 | 602 | 0.004 | 7.02 | 28 | -48 | -16 | Right fusiform gyrus |
| 0 | 892 | 0.017 | 6.37 | -26 | -80 | -10 | Left fusiform gyrus |
| 0 | 666 | 0.263 | 5.16 | -24 | -88 | 12 | Left middle occipital |
| 0.034 | 188 | 0.544 | 4.76 | -4 | 14 | 42 | Left middle cingulate gyrus |
| | | | | | | | |
| **EP Self, Negative** | | | | | | | |
| cluster | cluster | peak | peak | Coordinates | | | Region |
| p(FWE-corr) | size | p(FWE-corr) | T | x | y | z {mm} | |
| 0 | 621 | 0.118 | 5.38 | 6 | 48 | -4 | Right medial orbital gyrus |
| 0.009 | 346 | 0.172 | 5.21 | 48 | -54 | 28 | Right angular gyrus |
| | | | | | | | |
| **EP Self < EP Other** | | | | | | | |
| cluster | cluster | peak | peak | Coordinates | | | Region |
| p(FWE-corr) | size | p(FWE-corr) | T | x | y | z {mm} | |
| 0.026 | 229 | 0.249 | 5.12 | -24 | -54 | -14 | Left fusiform gyrus |
| | | | | | | | |
| **Risk, Other** | | | | | | | |
| cluster | cluster | peak | peak | Coordinates | | | Region |
| p(FWE-corr) | size | p(FWE-corr) | T | x | y | z {mm} | |
| 0.001 | 489 | 0.102 | 5.52 | -6 | 18 | 34 | Left middle cingulate gyrus |
| 0 | 533 | 0.143 | 5.37 | 28 | -6 | -4 | Right Putamen |
| 0 | 546 | 0.174 | 5.28 | -22 | 2 | 8 | Left Putamen |
| 0 | 968 | 0.179 | 5.27 | 26 | -86 | 12 | Right superior occipital |

| | | | | | | | |
|---|---|---|---|---|---|---|---|
| 0.015 | 266 | 0.259 | 5.09 | -54 | 6 | 26 | Left precentral gyrus |
| 0 | 537 | 0.397 | 4.87 | 16 | 4 | 54 | Right Frontal Superior |
| 0.017 | 258 | 0.436 | 4.81 | -12 | -98 | 12 | Leftoccipital pole |
| 0 | 579 | 0.449 | 4.8 | 16 | -82 | -14 | Right lingual gyrus |
| 0 | 581 | 0.453 | 4.79 | -28 | -66 | -22 | Left cerebellum exterior |
| 0 | 579 | 0.48 | 4.76 | 58 | -58 | -12 | Right inferior temporal gyrus |
| 0.007 | 312 | 0.685 | 4.5 | -14 | -68 | 52 | Left superior parietal lobule |
| | | | | | | | |
| Risk Self < Risk Other | | | | | | | |
| cluster | cluster | peak | peak | Coordinates | | | Region |
| p(FWE-corr) | size | p(FWE-corr) | T | x | y | z {mm} | |
| 0 | 575 | 0.147 | 5.35 | 64 | -48 | 2 | Right middle temporal gyrus |

**Table 3: Whole-Brain Neural Correlates of Post-Outcome Phase Variables** This table presents significant clusters of BOLD activity for pain intensity and surprise during the post-outcome phase of the task. Results are from a whole-brain random-effects analysis, thresholded at a voxel-level p<0.001 (uncorrected) and cluster-corrected at p<0.05 FWE, with a minimum cluster size (k) of 20 or 25 voxels (as indicated in the 'size' column for each contrast). Anatomical labels are derived from the AAL atlas.

| **Whole Brain, p = 0.001, k = 25** | | | | | | | |
|---|---|---|---|---|---|---|---|
| Pain S, FWE | | | | | | | |
| cluster | cluster | peak | peak | Coordinates | | | Region |
| p(FWE-corr) | size | p(FWE-corr) | T | x | y | z {mm} | |
| 0 | 891 | 0 | 9.69 | 0 | 8 | 34 | Left middle cingulate gyrus |
| 0 | 1780 | 0 | 8.88 | -42 | 6 | -6 | Left anterior insula |
| 0 | 380 | 0 | 8.15 | -54 | -30 | 30 | Left supramarginal gyrus |
| 0 | 1087 | 0 | 7.88 | 36 | 8 | 8 | Right anterior insula |
| 0 | 59 | 0.001 | 7.43 | 14 | -6 | 68 | Right supplementary motor area |
| 0 | 297 | 0.001 | 7.39 | 58 | -28 | 26 | Right parietal operculum |
| 0 | 116 | 0.001 | 7.28 | -8 | -16 | 70 | Left paracentral lobule |
| 0 | 65 | 0.002 | 6.96 | 6 | -36 | 0 | Right lingual gyrus |
| 0 | 86 | 0.003 | 6.84 | -18 | -48 | 66 | Left superior parietal lobule |
| 0.002 | 29 | 0.013 | 6.25 | 6 | -10 | 6 | Right thalamus |
| | | | | | | | |
| Pain Surprise Self | | | | | | | |
| cluster | cluster | peak | peak | Coordinates | | | Region |

| p(FWE -corr) | size | p(FWE-corr) | T | x | y | z {mm} | |
|---|---|---|---|---|---|---|---|
| 0.035 | 229 | 0.482 | 4.72 | 28 | -38 | 58 | Right postcentral gyrus |
| | | | | | | | |
| Pain Surprise S > Pain Surprise Other | | | | | | | |
| cluster | cluster | peak | peak | Coordinates | | | Region |
| p(FWE -corr) | size | p(FWE-corr) | T | x | y | z {mm} | |
| 0.023 | 260 | 0.272 | 5.03 | 28 | -38 | 58 | Right postcentral gyrus |

**Table 4: ROI Results for Predictive Phase Variables** This table presents significant BOLD responses within selected regions of interest (anterior insula, caudate, and putamen) during the predictive phase of the task. Results are from small volume corrected (SVC) analyses, with an underlying voxel threshold of p=0.01 (uncorrected) and corrected at p<0.05 FWE at the voxel level within the ROI. Anatomical labels are derived from the AAL atlas.

| **Threshold p = 0.01** | | | | | |
|---|---|---|---|---|---|
| **EP Self < EP Other** | | | | | |
| Left Caudate | | | | | |
| cluster | peak | peak | | | |
| size | p(FWE-corr) | T | x | y | z {mm} |
| 61 | 0.046 | 3.6 | -10 | 12 | 12 |
| | | | | | |
| **Risk, Self** | | | | | |
| Left Caudate | | | | | |
| cluster | peak | peak | Coordinates | | |
| size | p(FWE-corr) | T | x | y | z {mm} |
| 42 | 0.019 | 3.97 | -16 | 18 | 12 |
| 9 | 0.055 | 3.49 | -12 | 4 | 20 |
| | | | | | |
| **Risk, Other** | | | | | |
| Left Anterior Insula | | | | | |
| cluster | peak | peak | coordinates | | |
| size | p(FWE-corr) | T | x | y | z {mm} |
| 217 | 0.028 | 3.96 | -44 | 4 | -6 |
| | | | | | |
| Right Anterior Insula | | | | | |
| cluster | peak | peak | coordinates | | |
| size | p(FWE-corr) | T | x | y | z {mm} |
| 99 | 0.034 | 3.86 | 36 | 6 | 4 |

| | | | | | |
|---|---|---|---|---|---|
| | | | | | |
| Left Caudate | | | | | |
| cluster | peak | peak | coordinates | | |
| size | p(FWE-corr) | T | x | y | z {mm} |
| 231 | 0.005 | 4.58 | -14 | 2 | 18 |
| | 0.013 | 4.16 | -14 | -10 | 20 |
| | | | | | |
| Right Caudate | | | | | |
| cluster | peak | peak | Coordinates | | |
| size | p(FWE-corr) | T | x | y | z {mm} |
| 180 | 0.004 | 4.69 | 18 | 2 | 16 |
| | 0.004 | 4.65 | 14 | 6 | 10 |
| | | | | | |
| Left Putamen | | | | | |
| cluster | peak | peak | Coordinates | | |
| size | p(FWE-corr) | T | x | y | z {mm} |
| 486 | 0.001 | 5.28 | -22 | 2 | 8 |
| | 0.021 | 4.02 | -28 | 0 | -6 |
| | 0.033 | 3.82 | -28 | 8 | -4 |
| | | | | | |
| Right Putamen | | | | | |
| cluster | peak | peak | Coordinates | | |
| size | p(FWE-corr) | T | x | y | z {mm} |
| 371 | 0.001 | 5.37 | 28 | -6 | -4 |
| | 0.012 | 4.27 | 22 | 2 | 8 |
| | | | | | |
| **Risk Self < Risk Other** | | | | | |
| Left Anterior Insula | | | | | |
| cluster | peak | peak | coordinates | | |
| size | p(FWE-corr) | T | x | y | z {mm} |
| 63 | 0.022 | 4.05 | -44 | 4 | -8 |
| | | | | | |
| Right Putamen | | | | | |
| cluster | peak | peak | coordinates | | |
| size | p(FWE-corr) | T | x | y | z {mm} |
| 150 | 0.041 | 3.71 | 28 | -10 | -6 |

**Table 5: ROI Results for Post-Outcome Phase Variables** This table presents significant BOLD responses within selected regions of interest (anterior insula, caudate) during the post-outcome phase of the task. Results

are from small volume corrected (SVC) analyses, with an underlying voxel threshold of p=0.01 (uncorrected) and corrected at p<0.05 FWE at the voxel level within the ROI.

| **Threshold p = 0.01** | | | | | |
|---|---|---|---|---|---|
| **Pain, Other** | | | | | |
| Right anterior insula | | | | | |
| cluster | peak | peak | Coordinates | | |
| size | p(FWE-corr) | T | x | y | z {mm} |
| 183 | 0.026 | 3.86 | 38 | 14 | 0 |
| | | | | | |
| **Pain Other, Negative** | | | | | |
| Left Caudate | | | | | |
| cluster | peak | peak | | | |
| size | p(FWE-corr) | T | x | y | z {mm} |
| 23 | 0.036 | 3.59 | -10 | 20 | 6 |
| | | | | | |
| Right Caudate | | | | | |
| cluster | peak | peak | | | |
| size | p(FWE-corr) | T | x | y | z {mm} |
| 30 | 0.02 | 3.87 | 18 | 24 | 6 |
| | 0.021 | 3.84 | 16 | 24 | 2 |
| | | | | | |
| **Pain Surprise, Self** | | | | | |
| Right Anterior Insula (Surprise Peak) | | | | | |
| cluster | peak | peak | Coordinates | | |
| size | p(FWE-corr) | T | x | y | z {mm} |
| 121 | 0.016 | 3.9 | 48 | 26 | -10 |
| | 0.027 | 3.66 | 36 | 28 | -16 |
| | | | | | |
| Pain Surprise, Other | | | | | |
| Right Anterior Insula (Surprise Peak) | | | | | |
| cluster | peak | peak | Coordinates | | |
| size | p(FWE-corr) | T | x | y | z {mm} |
| 77 | 0.039 | 3.43 | 44 | 26 | -2 |

Acknowledgments: This study is funded by the Swiss National Science Foundation grant PP00P1_183715 awarded to CCD.

References

(1) Song, Y.; Yao, M.; Kemprecos, H.; Byrne, A.; Xiao, Z.; Zhang, Q.; Singh, A.; Wang, J.; Chen, Z. Predictive Coding Models for Pain Perception. *Journal of Computational Neuroscience* **2021**, *49*, 1–21. https://doi.org/10.1007/s10827-021-00780-x.

(2) Büchel, C.; Geuter, S.; Sprenger, C.; Eippert, F. Placebo Analgesia: A Predictive Coding Perspective. *Neuron* **2014**, *81* (6), 1223–1239. https://doi.org/10.1016/j.neuron.2014.02.042.

(3) Lersch, F. E.; Frickmann, F. C. S.; Urman, R. D.; Burgermeister, G.; Siercks, K.; Luedi, M. M.; Straumann, S. Analgesia for the Bayesian Brain: How Predictive Coding Offers Insights Into the Subjectivity of Pain. *Curr Pain Headache Rep* **2023**, *27* (11), 631–638. https://doi.org/10.1007/s11916-023-01122-5.

(4) Brown, C. A.; Seymour, B.; El-Deredy, W.; Jones, A. K. P. Confidence in Beliefs about Pain Predicts Expectancy Effects on Pain Perception and Anticipatory Processing in Right Anterior Insula. *PAIN* **2008**, *139* (2), 324–332. https://doi.org/10.1016/j.pain.2008.04.028.

(5) Clark, J. A.; Brown, C. A.; Jones, A. K. P.; El-Deredy, W. Dissociating Nociceptive Modulation by the Duration of Pain Anticipation from Unpredictability in the Timing of Pain. *Clinical Neurophysiology* **2008**, *119* (12), 2870–2878. https://doi.org/10.1016/j.clinph.2008.09.022.

(6) Zaman, J.; Van Oudenhove, L.; Vlaeyen, J. W. S. Uncertainty in a Context of Pain: Disliked but Also More Painful? *PAIN* **2021**, *162* (4), 995–998. https://doi.org/10.1097/j.pain.0000000000002106.

(7) Pavy, F.; Zaman, J.; Van den Noortgate, W.; Scarpa, A.; von Leupoldt, A.; Torta, D. M. The Effect of Unpredictability on the Perception of Pain: A Systematic Review and Meta-Analysis. *PAIN* **2024**, *165* (8), 1702. https://doi.org/10.1097/j.pain.0000000000003199.

(8) Seymour, B. Pain: A Precision Signal for Reinforcement Learning and Control. *Neuron* **2019**, *101* (6), 1029–1041. https://doi.org/10.1016/j.neuron.2019.01.055.

(9) Strube, A.; Horing, B.; Rose, M.; Büchel, C. Agency Affects Pain Inference through Prior Shift as Opposed to Likelihood Precision Modulation in a Bayesian Pain Model. *Neuron* **2023**, *111* (7), 1136-1151.e7. https://doi.org/10.1016/j.neuron.2023.01.002.

(10) Mellers, B.; Fincher, K.; Drummond, C.; Bigony, M. Chapter 1 - Surprise: A Belief or an Emotion? In *Progress in Brain Research*; Pammi, V. S. C., Srinivasan, N., Eds.; Decision Making; Elsevier, 2013; Vol. 202, pp 3–19. https://doi.org/10.1016/B978-0-444-62604-2.00001-0.

(11) Lockwood, P. L.; Wittmann, M. K.; Apps, M. A. J.; Klein-Flügge, M. C.; Crockett, M. J.; Humphreys, G. W.; Rushworth, M. F. S. Neural Mechanisms for Learning Self and Other Ownership. *Nature Communications* **2018**, *9* (1), 1–11. https://doi.org/10.1038/s41467-018-07231-9.

(12) Barnby, J. M.; Raihani, N.; Dayan, P. The Self as a Prior for the Other: Social Learning under Paranoia. PsyArXiv September 21, 2021. https://doi.org/10.31234/osf.io/an5kp.

(13) McGovern, H. T.; Otten, M. Priors and Prejudice: Hierarchical Predictive Processing in Intergroup Perception. *Front. Psychol.* **2024**, *15*. https://doi.org/10.3389/fpsyg.2024.1386370.

(14) Peter, E.; Watt-Watson, J. Unrelieved Pain: An Ethical and Epistemological Analysis of Distrust in Patients. *Canadian Journal of Nursing Research Archive* **2002**.

(15) Dirupo, G.; Totaro, S.; Richard, J.; Corradi-Dell'Acqua, C. Medical Education and Distrust Modulate the Response of Insular-Cingulate Network and Ventral Striatum in Pain Diagnosis. *Elife* **2021**, *10*, e63272. https://doi.org/10.7554/eLife.63272.

(16) Mishra, S. Decision-Making Under Risk: Integrating Perspectives From Biology, Economics, and Psychology. *Pers Soc Psychol Rev* **2014**, *18* (3), 280–307. https://doi.org/10.1177/1088868314530517.
(17) Trepel, C.; Fox, C. R.; Poldrack, R. A. Prospect Theory on the Brain? Toward a Cognitive Neuroscience of Decision under Risk. *Cognitive Brain Research* **2005**, *23* (1), 34–50. https://doi.org/10.1016/j.cogbrainres.2005.01.016.
(18) Stone, E. R.; YoonSun, C.; Bruine de Bruin, W.; Mandel, D. R. I Can Take the Risk, but You Should Be Safe: Self-Other Differences in Situations Involving Physical Safety. *Judgment and Decision Making* **2013**, *8* (3), 250–267.
(19) Loued-Khenissi, L.; Martin-Brevet, S.; Schumacher, L.; Corradi-Dell'Acqua, C. The Effect of Uncertainty on Pain Decisions for Self and Others. *European Journal of Pain* **2022**, *26* (5), 1163–1175. https://doi.org/10.1002/ejp.1940.
(20) Kahneman, D.; Tversky, A. Prospect Theory: An Analysis of Decision under Risk. *Econometrica* **1979**, *47* (2), 263–291.
(21) Loued-Khenissi, L.; Corradi-Dell'Acqua, C. Gambling on Others' Health: Risky pro-Social Decision-Making in the Era of COVID-19. *Front. Psychol.* **2024**, *15*. https://doi.org/10.3389/fpsyg.2024.1370778.
(22) Polman, E.; Wu, K. Decision Making for Others Involving Risk: A Review and Meta-Analysis. *Journal of Economic Psychology* **2020**, *77*, 102184. https://doi.org/10.1016/j.joep.2019.06.007.
(23) Loued-Khenissi, L.; Martin-Brevet, S.; Schumacher, L.; Corradi-Dell'Acqua, C. The Effect of Uncertainty on Pain Decisions for Self and Others. *European Journal of Pain* **2022**, *26* (5), 1163–1175. https://doi.org/10.1002/ejp.1940.
(24) Yoshida, W.; Seymour, B.; Koltzenburg, M.; Dolan, R. J. Uncertainty Increases Pain: Evidence for a Novel Mechanism of Pain Modulation Involving the Periaqueductal Gray. *J. Neurosci.* **2013**, *33* (13), 5638–5646. https://doi.org/10.1523/JNEUROSCI.4984-12.2013.
(25) Preuschoff, K.; Bossaerts, P.; Quartz, S. R. Neural Differentiation of Expected Reward and Risk in Human Subcortical Structures. *Neuron* **2006**, *51* (3), 381–390. https://doi.org/10.1016/j.neuron.2006.06.024.
(26) Knutson, B.; Huettel, S. A. The Risk Matrix. *Current Opinion in Behavioral Sciences* **2015**, *5*, 141–146. https://doi.org/10.1016/j.cobeha.2015.10.012.
(27) Tobler, P. N.; O'Doherty, J. P.; Dolan, R. J.; Schultz, W. Reward Value Coding Distinct From Risk Attitude-Related Uncertainty Coding in Human Reward Systems. *Journal of Neurophysiology* **2006**, *97* (2), 1621–1632. https://doi.org/10.1152/jn.00745.2006.
(28) Jones, C. L.; Minati, L.; Harrison, N. A.; Ward, J.; Critchley, H. D. Under Pressure: Response Urgency Modulates Striatal and Insula Activity during Decision-Making under Risk. *PLoS ONE* **2011**, *6* (6). https://doi.org/10.1371/journal.pone.0020942.
(29) Preuschoff, K.; Quartz, S. R.; Bossaerts, P. Human Insula Activation Reflects Risk Prediction Errors as Well as Risk. *The Journal of neuroscience : the official journal of the Society for Neuroscience* **2008**, *28* (11), 2745–2752. https://doi.org/10.1523/JNEUROSCI.4286-07.2008.
(30) Mohr, P. N. C.; Biele, G.; Heekeren, H. R. Neural Processing of Risk. *The Journal of neuroscience : the official journal of the Society for Neuroscience* **2010**, *30* (19), 6613–6619. https://doi.org/10.1523/JNEUROSCI.0003-10.2010.
(31) Sun, C.; Qian, H.; Miao, C. From Psychological Curiosity to Artificial Curiosity: Curiosity-Driven Learning in Artificial Intelligence Tasks. arXiv January 20, 2022. https://doi.org/10.48550/arXiv.2201.08300.

(32) Loued-Khenissi, L.; Pfeuffer, A.; Einhäuser, W.; Preuschoff, K. Anterior Insula Reflects Surprise in Value-Based Decision-Making and Perception. *NeuroImage* **2020**, 116549. https://doi.org/10.1016/j.neuroimage.2020.116549.
(33) Fazeli, S.; Büchel, C. Pain-Related Expectation and Prediction Error Signals in the Anterior Insula Are Not Related to Aversiveness. *J. Neurosci.* **2018**, *38* (29), 6461–6474. https://doi.org/10.1523/JNEUROSCI.0671-18.2018.
(34) Lutz, A.; McFarlin, D. R.; Perlman, D. M.; Salomons, T. V.; Davidson, R. J. Altered Anterior Insula Activation during Anticipation and Experience of Painful Stimuli in Expert Meditators. *NeuroImage* **2013**, *64*, 538–546. https://doi.org/10.1016/j.neuroimage.2012.09.030.
(35) Isnard, J.; Magnin, M.; Jung, J.; Mauguière, F.; Garcia-Larrea, L. Does the Insula Tell Our Brain That We Are in Pain? *PAIN*® **2011**, *152* (4), 946–951. https://doi.org/10.1016/j.pain.2010.12.025.
(36) Moayedi, M. All Roads Lead to the Insula. *PAIN* **2014**, *155* (10), 1920. https://doi.org/10.1016/j.pain.2014.07.023.
(37) Corradi-Dell'Acqua, C.; Tusche, A.; Vuilleumier, P.; Singer, T. Cross-Modal Representations of First-Hand and Vicarious Pain, Disgust and Fairness in Insular and Cingulate Cortex. *Nat Commun* **2016**, *7* (1), 1–12. https://doi.org/10.1038/ncomms10904.
(38) Fields, H. L. How Expectations Influence Pain. *PAIN* **2018**, *159*, S3. https://doi.org/10.1097/j.pain.0000000000001272.
(39) Atlas, L. Y.; Wager, T. D. How Expectations Shape Pain. *Neuroscience Letters* **2012**, *520* (2), 140–148. https://doi.org/10.1016/j.neulet.2012.03.039.
(40) Peerdeman, K. J.; van Laarhoven, A. I. M.; Keij, S. M.; Vase, L.; Rovers, M. M.; Peters, M. L.; Evers, A. W. M. Relieving Patients' Pain with Expectation Interventions: A Meta-Analysis. *PAIN* **2016**, *157* (6), 1179. https://doi.org/10.1097/j.pain.0000000000000540.
(41) Hoskin, R.; Berzuini, C.; Acosta-Kane, D.; El-Deredy, W.; Guo, H.; Talmi, D. Sensitivity to Pain Expectations: A Bayesian Model of Individual Differences. *Cognition* **2019**, *182*, 127–139. https://doi.org/10.1016/j.cognition.2018.08.022.
(42) Büchel, C. The Role of Expectations, Control and Reward in the Development of Pain Persistence Based on a Unified Model. *eLife* **2023**, *12*, e81795. https://doi.org/10.7554/eLife.81795.
(43) Song, Y.; Kemprecos, H.; Wang, J.; Chen, Z. A Predictive Coding Model for Evoked and Spontaneous Pain Perception. In *2019 41st Annual International Conference of the IEEE Engineering in Medicine and Biology Society (EMBC)*; 2019; pp 2964–2967. https://doi.org/10.1109/EMBC.2019.8857298.
(44) Tabor, A.; Burr, C. Bayesian Learning Models of Pain: A Call to Action. *Curr. Opin. Behav. Sci.* **2019**, *26*, 54–61. https://doi.org/10.1016/j.cobeha.2018.10.006.
(45) Prkachin, K. M.; Solomon, P. E.; Ross, J. Underestimation of Pain by Health-Care Providers: Towards a Model of the Process of Inferring Pain in Others. *Canadian Journal of Nursing Research Archive* **2007**, 88–106.
(46) Kappesser, J.; Williams, A. C. de C.; Prkachin, K. M. Testing Two Accounts of Pain Underestimation. *Pain* **2006**, *124* (1), 109–116. https://doi.org/10.1016/j.pain.2006.04.003.
(47) Seers, T.; Derry, S.; Seers, K.; Moore, R. A. Professionals Underestimate Patients' Pain: A Comprehensive Review. *Pain* **2018**, *159* (5), 811–818. https://doi.org/10.1097/j.pain.0000000000001165.
(48) Bonnet, C.; Fauquet Ars, J.; Estaún Ferrer, S. Reaction Times as a Measure of Uncertainty. *Psicothema* **2008**, *20* (1), 43–48.

(49) Batson, C. D. *Altruism in Humans*; Oxford University Press, 2010.
(50) Hutcherson, C. A.; Bushong, B.; Rangel, A. A Neurocomputational Model of Altruistic Choice and Its Implications. *Neuron* **2015**, *87* (2), 451–462. https://doi.org/10.1016/j.neuron.2015.06.031.
(51) Fehr, E.; Rockenbach, B. Human Altruism: Economic, Neural, and Evolutionary Perspectives. *Current Opinion in Neurobiology* **2004**, *14* (6), 784–790. https://doi.org/10.1016/j.conb.2004.10.007.
(52) Cui, F.; Abdelgabar, A.-R.; Keysers, C.; Gazzola, V. Responsibility Modulates Pain-Matrix Activation Elicited by the Expressions of Others in Pain. *NeuroImage* **2015**, *114*, 371–378. https://doi.org/10.1016/j.neuroimage.2015.03.034.
(53) Lepron, E.; Causse, M.; Farrer, C. Responsibility and the Sense of Agency Enhance Empathy for Pain. *Proceedings of the Royal Society B: Biological Sciences* **2015**, *282* (1799), 20142288. https://doi.org/10.1098/rspb.2014.2288.
(54) Pu, M.; Yu, R. Personal Responsibility Modulates Neural Representations of Anticipatory and Experienced Pain. *Psychophysiology* **2019**, *56* (3), e13294. https://doi.org/10.1111/psyp.13294.
(55) Williams, D. A.; Robinson, M. E.; Geisser, M. E. Pain Beliefs: Assessment and Utility. *Pain* **1994**, *59* (1), 71–78. https://doi.org/10.1016/0304-3959(94)90049-3.
(56) Pariente, J.; White, P.; Frackowiak, R. S. J.; Lewith, G. Expectancy and Belief Modulate the Neuronal Substrates of Pain Treated by Acupuncture. *NeuroImage* **2005**, *25* (4), 1161–1167. https://doi.org/10.1016/j.neuroimage.2005.01.016.
(57) Wiech, K.; Lin, C.; Brodersen, K. H.; Bingel, U.; Ploner, M.; Tracey, I. Anterior Insula Integrates Information about Salience into Perceptual Decisions about Pain. *J. Neurosci.* **2010**, *30* (48), 16324. https://doi.org/10.1523/JNEUROSCI.2087-10.2010.
(58) Lamm, C.; Decety, J.; Singer, T. Meta-Analytic Evidence for Common and Distinct Neural Networks Associated with Directly Experienced Pain and Empathy for Pain. *NeuroImage* **2011**, *54* (3), 2492–2502. https://doi.org/10.1016/j.neuroimage.2010.10.014.
(59) Treue, S. Visual Attention: The Where, What, How and Why of Saliency. *Current Opinion in Neurobiology* **2003**, *13* (4), 428–432. https://doi.org/10.1016/S0959-4388(03)00105-3.
(60) Birmingham, E.; Bischof, W. F.; Kingstone, A. Social Attention and Real-World Scenes: The Roles of Action, Competition and Social Content. *Quarterly Journal of Experimental Psychology* **2008**, *61* (7), 986–998. https://doi.org/10.1080/17470210701410375.
(61) Krishnan, A.; Woo, C.-W.; Chang, L. J.; Ruzic, L.; Gu, X.; López-Solà, M.; Jackson, P. L.; Pujol, J.; Fan, J.; Wager, T. D. Somatic and Vicarious Pain Are Represented by Dissociable Multivariate Brain Patterns. *eLife* **2016**, *5*, e15166. https://doi.org/10.7554/eLife.15166.
(62) Siman-Tov, T.; Granot, R. Y.; Shany, O.; Singer, N.; Hendler, T.; Gordon, C. R. Is There a Prediction Network? Meta-Analytic Evidence for a Cortical-Subcortical Network Likely Subserving Prediction. *Neurosci Biobehav Rev* **2019**, *105*, 262–275. https://doi.org/10.1016/j.neubiorev.2019.08.012.
(63) Padoa-Schioppa, C.; Assad, J. A. Neurons in the Orbitofrontal Cortex Encode Economic Value. *Nature* **2006**, *441* (7090), 223–226. https://doi.org/10.1038/nature04676.
(64) Palermo, S.; Benedetti, F.; Costa, T.; Amanzio, M. Pain Anticipation: An Activation Likelihood Estimation Meta-Analysis of Brain Imaging Studies. *Human Brain Mapping* **2015**, *36* (5), 1648–1661. https://doi.org/10.1002/hbm.22727.
(65) R, G.; C, S.; S, B.; Ag, M.; Td, W.; M, R. Neurophysiological Encoding of Aversive Prediction Errors. *Pain* **2025**. https://doi.org/10.1097/j.pain.0000000000003712.

(66) Tom, S. M.; Fox, C. R.; Trepel, C.; Poldrack, R. a. The Neural Basis of Loss Aversion in Decision-Making under Risk. *Science (New York, N.Y.)* **2007**, *315* (5811), 515–518. https://doi.org/10.1126/science.1134239.
(67) Lockwood, P. L.; Apps, M. A. J.; Roiser, J. P.; Viding, E. Encoding of Vicarious Reward Prediction in Anterior Cingulate Cortex and Relationship with Trait Empathy. *J. Neurosci.* **2015**, *35* (40), 13720–13727. https://doi.org/10.1523/JNEUROSCI.1703-15.2015.
(68) Alexander, W. H.; Brown, J. W. A General Role for Medial Prefrontal Cortex in Event Prediction. **2014**, *8* (July), 1–11. https://doi.org/10.3389/fncom.2014.00069.
(69) Monosov, I. E. Anterior Cingulate Is a Source of Valence-Specific Information about Value and Uncertainty. *Nat Commun* **2017**, *8* (1), 134. https://doi.org/10.1038/s41467-017-00072-y.
(70) Ide, J. S.; Shenoy, P.; Yu, A. J.; Li, C. R. Bayesian Prediction and Evaluation in the Anterior Cingulate Cortex. **2013**, *33* (5), 2039–2047. https://doi.org/10.1523/JNEUROSCI.2201-12.2013.
(71) Korucuoglu, O.; Harms, M. P.; Astafiev, S. V.; Kennedy, J. T.; Golosheykin, S.; Barch, D. M.; Anokhin, A. P. Test-Retest Reliability of fMRI-Measured Brain Activity during Decision Making under Risk. *NeuroImage* **2020**, *214*, 116759. https://doi.org/10.1016/j.neuroimage.2020.116759.
(72) Brown, C. A.; Seymour, B.; Boyle, Y.; El-Deredy, W.; Jones, A. K. P. Modulation of Pain Ratings by Expectation and Uncertainty: Behavioral Characteristics and Anticipatory Neural Correlates. *PAIN* **2008**, *135* (3), 240–250. https://doi.org/10.1016/j.pain.2007.05.022.
(73) Sharvit, G.; Corradi-Dell'Acqua, C.; Vuilleumier, P. Modality-Specific Effects of Aversive Expectancy in the Anterior Insula and Medial Prefrontal Cortex. *Pain* **2018**, *159* (8), 1529–1542. https://doi.org/10.1097/j.pain.0000000000001237.
(74) Sharvit, G.; Vuilleumier, P.; Corradi-Dell'Acqua, C. Sensory-Specific Predictive Models in the Human Anterior Insula. F1000Research February 6, 2019. https://doi.org/10.12688/f1000research.17961.1.
(75) Geuter, S.; Boll, S.; Eippert, F.; Büchel, C. Functional Dissociation of Stimulus Intensity Encoding and Predictive Coding of Pain in the Insula. *eLife* **2017**, *6*, e24770. https://doi.org/10.7554/eLife.24770.
(76) Hoskin, R.; Talmi, D. Adaptive Coding of Pain Prediction Error in the Anterior Insula. *European Journal of Pain* **2023**, *27* (6), 766–778. https://doi.org/10.1002/ejp.2093.
(77) Kiverstein, J.; Kirchhoff, M. D.; Thacker, M. An Embodied Predictive Processing Theory of Pain Experience. *Rev.Phil.Psych.* **2022**, *13* (4), 973–998. https://doi.org/10.1007/s13164-022-00616-2.
(78) Zaki, J.; Wager, T. D.; Singer, T.; Keysers, C.; Gazzola, V. The Anatomy of Suffering: Understanding the Relationship between Nociceptive and Empathic Pain. *Trends in Cognitive Sciences* **2016**, *20* (4), 249–259. https://doi.org/10.1016/j.tics.2016.02.003.
(79) Pereda, M.; Brañas-Garza, P.; Rodríguez-Lara, I.; Sánchez, A. The Emergence of Altruism as a Social Norm. *Sci Rep* **2017**, *7* (1), 9684. https://doi.org/10.1038/s41598-017-07712-9.
(80) Andreoni, J.; Rao, J. M.; Trachtman, H. Avoiding the Ask: A Field Experiment on Altruism, Empathy, and Charitable Giving. *Journal of Political Economy* **2017**, *125* (3), 625–653. https://doi.org/10.1086/691703.
(81) Asakura, N.; Inui, T. A Bayesian Framework for False Belief Reasoning in Children: A Rational Integration of Theory-Theory and Simulation Theory. *Front. Psychol.* **2016**, *7*. https://doi.org/10.3389/fpsyg.2016.02019.

(82) Morrison, G. C. WTP and WTA in Repeated Trial Experiments: Learning or Leading? *Journal of Economic Psychology* **2000**, *21* (1), 57–72. https://doi.org/10.1016/S0167-4870(99)00036-7.
(83) Benuzzi, F.; Lui, F.; Ardizzi, M.; Ambrosecchia, M.; Ballotta, D.; Righi, S.; Pagnoni, G.; Gallese, V.; Porro, C. A. Pain Mirrors: Neural Correlates of Observing Self or Others' Facial Expressions of Pain. *Front. Psychol.* **2018**, *9*. https://doi.org/10.3389/fpsyg.2018.01825.
(84) Lang, S.; Yu, T.; Markl, A.; Müller, F.; Kotchoubey, B. Hearing Others' Pain: Neural Activity Related to Empathy. *Cogn Affect Behav Neurosci* **2011**, *11* (3), 386–395. https://doi.org/10.3758/s13415-011-0035-0.
(85) Boring, B. L.; Ng, B. W.; Nanavaty, N.; Mathur, V. A. Over-Rating Pain Is Overrated: A Fundamental Self-Other Bias in Pain Reporting Behavior. *The Journal of Pain* **2022**, *23* (10), 1779–1789. https://doi.org/10.1016/j.jpain.2022.06.002.
(86) Preuschoff, K.; 't Hart, B. M.; Einhäuser, W. Pupil Dilation Signals Surprise: Evidence for Noradrenaline's Role in Decision Making. *Frontiers in neuroscience* **2011**, *5* (September), 115. https://doi.org/10.3389/fnins.2011.00115.
(87) Eklund, A.; Nichols, T.; Knutsson, H. Can Parametric Statistical Methods Be Trusted for fMRI Based Group Studies? *Proc Natl Acad Sci USA* **2016**, *113* (28), 7900–7905. https://doi.org/10.1073/pnas.1602413113.